

Reactions of Germanium Atoms and Small Clusters with CO: Experimental and Theoretical Characterization of Ge_nCO ($n = 1-5$) and $\text{Ge}_2(\text{CO})_2$ in Solid Argon

Mingfei Zhou,^{*,†} Ling Jiang,[‡] and Qiang Xu^{*,‡}

Department of Chemistry & Laser Chemistry Institute, Shanghai Key Laboratory of Molecular Catalysts and Innovative Materials, Fudan University, Shanghai 200433, P.R.C., and National Institute of Advanced Industrial Science and Technology (AIST), Ikeda, Osaka 563-8577, Japan

Received: December 1, 2004; In Final Form: February 19, 2005

Reactions of germanium atoms and small clusters with carbon monoxide molecules in solid argon have been studied using matrix isolation infrared absorption spectroscopy. Besides the previously reported GeCO monocarbonyl, the $\text{Ge}_2(\text{CO})_2$ and Ge_nCO ($n = 2-5$) carbonyl molecules are formed spontaneously on annealing and are characterized on the basis of isotopic substitution and theoretical calculations. It is found that Ge_2CO , Ge_3CO , and Ge_5CO are bridge-bonded carbonyl compounds, whereas $\text{Ge}_2(\text{CO})_2$ and Ge_4CO are terminal-bonded carbonyl molecules.

Introduction

Small silicon and germanium clusters have been the subject of a number of theoretical and experimental studies both because of their intrinsic interest from the viewpoint of chemical structure and bonding and because of the potential technological applications of microelectronic devices and the high-tech industry. A number of experimental techniques have been employed to study the germanium clusters. Laser photoelectron spectroscopy of negative ions has been used for the determination of adiabatic electron affinities and electronic structures of mass-selected clusters. Following the work of Smalley and co-workers on the anion photoelectron spectroscopy of Ge_n^- ($n = 3-12$),¹ Neumark's group has reported photoelectron and zero electron kinetic energy spectroscopic studies of Ge_n^- ($n = 2-15$).^{2,3} Besides the electron affinities of the neutral clusters, the vibrational frequencies for several electronic states of Ge_2 and Ge_3 were determined. Froben and Schulze have obtained the Raman and fluorescence spectra of cryogenic matrix isolated Ge_n clusters ($n = 2-4$).⁴ Weltner and co-workers have obtained the magneto-infrared spectra of Ge_2 in rare gas matrixes.⁵ Ab initio quantum chemical calculations have also been used to determine the geometries, electronic structures, and binding energies of germanium clusters.⁶⁻¹² It has been established that Ge_2 has a $^3\Sigma_g^-$ ground state with a low-lying $^3\Pi_u$ state. The Ge_3 trimer has a 1A_1 ground state with C_{2v} symmetry. A 1A_g ground state with planar rhombus D_{2h} symmetry has been predicted for Ge_4 , and the ground state of Ge_5 has been found to be 1A_1 of D_{3h} symmetry.

The reactions of small clusters with molecules such as CO, H_2 , NH_3 , and H_2O are usually used to gain insight into their chemisorption characteristics and catalytic activity. Many studies of the chemical reactions of silicon clusters with water, ammonia, acetylene, and carbon monoxide have been performed,¹³⁻¹⁵ but much less is known about the reactivity of the germanium clusters. An early study on the reaction of

germanium atoms and carbon monoxide in solid matrix has characterized the germanium carbonyl species: GeCO and $\text{Ge}(\text{CO})_2$.¹⁶ The ground state of GeCO was determined to be $^3\Sigma^-$. The $\text{Ge}(\text{CO})_2$ molecule was predicted to have a singlet ground state with a bent C_{2v} symmetry.¹⁷ Recently, small silicon cluster carbonyls Si_nCO ($n = 1-5$) and $\text{Si}_2(\text{CO})_2$ have been synthesized in solid argon matrix using the technique of laser ablation coupled with matrix isolation. The spectra, structures, bonding, and reactivity of these small silicon cluster carbonyl species were obtained.¹⁸ In this paper, we report a similar study on the germanium carbonyl species $\text{Ge}_n(\text{CO})$ ($n = 1-5$) and $\text{Ge}_2(\text{CO})_2$ formed from the reactions of germanium atoms and small clusters with CO in solid argon.

Experimental and Computational Methods

The experiment for laser ablation and matrix isolation infrared spectroscopy is similar to those reported previously.¹⁹ Briefly, the Nd:YAG laser fundamental (1064 nm, 10 Hz repetition rate with 10-ns pulse width) was focused on a rotating germanium target. The laser-ablated germanium atoms and clusters were co-deposited with CO in excess argon onto a CsI window cooled normally to 7 K by means of a closed-cycle helium refrigerator. The matrix gas deposition rate was typically of 2–4 mmol per hour. Carbon monoxide (99.95%), $^{13}\text{C}^{16}\text{O}$ (99%, $^{18}\text{O} < 1\%$), and $^{12}\text{C}^{18}\text{O}$ (99%) were used to prepare the CO/Ar mixtures. In general, matrix samples were deposited for 1–2 h. After sample deposition, IR spectra were recorded on a BIO-RAD FTS-6000e spectrometer at 0.5 cm^{-1} resolution using a liquid-nitrogen-cooled HgCdTe (MCT) detector for the spectral range of 5000–400 cm^{-1} . Samples were annealed at different temperatures and subjected to broadband irradiation ($\lambda > 250\text{ nm}$) using a high-pressure mercury arc lamp (Ushio, 100 W).

Quantum chemical calculations were performed to predict the structures and vibrational frequencies of the observed reaction products using the Gaussian 03 program.²⁰ The Becke three-parameter hybrid functional with the Lee–Yang–Parr correlation corrections (B3LYP) was used.^{21,22} The 6-311+G* basis sets were used for Ge, C, and O atoms.²³ Geometries were fully optimized and vibrational frequencies were calculated with analytical second derivatives.

* Corresponding authors. E-mail: mzfzhou@fudan.edu.cn (Zhou), q.xu@aist.go.jp (Xu).

[†] Fudan University.

[‡] National Institute of Advanced Industrial Science and Technology (AIST).

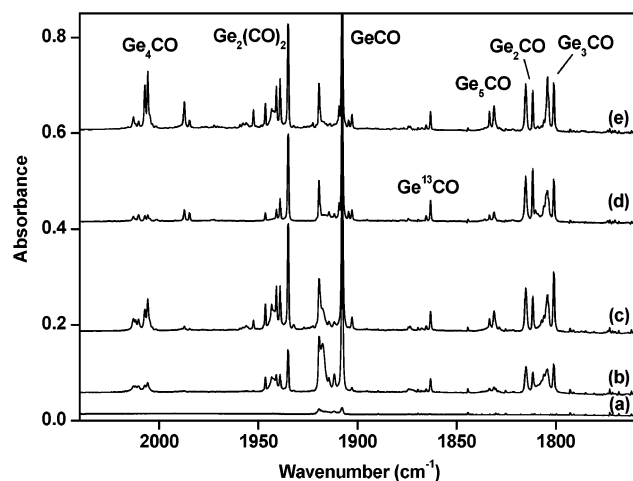


Figure 1. Infrared spectra in the 2040–1760 cm^{-1} region from co-deposition of laser-ablated germanium atoms with 0.025% CO in Ar. (a) 1 h of sample deposition at 7 K, (b) after annealing to 30 K, (c) after annealing to 34 K, (d) after 20 min of broad-band irradiation, and (e) after annealing to 38 K.

TABLE 1: Infrared Absorptions (cm^{-1}) from Co-deposition of Laser-Ablated Germanium Atoms with CO in Excess Argon

$^{12}\text{C}^{16}\text{O}$	$^{13}\text{C}^{16}\text{O}$	$^{12}\text{C}^{18}\text{O}$	$R(^{12}\text{C}/^{13}\text{C})$	$R(^{16}\text{O}/^{18}\text{O})$	assignment
2007.2	1963.2	1959.2	1.0224	1.0245	Ge_4CO site
2005.7	1961.8	1957.8	1.0224	1.0245	Ge_4CO
1987.3	1943.0	1941.2	1.0228	1.0237	$\text{Ge}_x(\text{CO})_y$
1984.7	1940.4	1938.8	1.0228	1.0237	$\text{Ge}_x(\text{CO})_y$ site
1952.5	1910.1	1905.5	1.0222	1.0247	$\text{Ge}_2(\text{CO})_2$ site
1946.4	1904.6	1899.0	1.0219	1.0250	$\text{Ge}_2(\text{CO})_2$ site
1940.9	1899.2	1893.5	1.0220	1.0250	$\text{Ge}_2(\text{CO})_2$ site
1939.0	1897.3	1891.6	1.0220	1.0251	$\text{Ge}_2(\text{CO})_2$ site
1935.0	1893.4	1887.6	1.0220	1.0251	$\text{Ge}_2(\text{CO})_2$
1919.3	1876.9	1874.3	1.0226	1.0240	GeCO site
1907.7	1865.4	1863.1	1.0227	1.0239	GeCO
1833.5	1793.6	1787.7	1.0222	1.0256	Ge_5CO site
1831.2	1791.4	1785.8	1.0222	1.0254	Ge_5CO
1815.2	1774.7	1773.6	1.0228	1.0235	Ge_2CO site
1811.7	1771.3	1770.1	1.0228	1.0235	Ge_2CO
1804.2	1765.0	1760.7	1.0222	1.0247	Ge_3CO site
1801.0	1761.8	1757.5	1.0222	1.0248	Ge_3CO

Results and Discussions

Infrared Spectra. A series of experiments has been done using various CO concentrations (ranging from 0.025 to 0.5% in argon) and various laser energies (ranging from 3 to 8 mJ/pulse) to control the relative concentrations of Ge and CO. The infrared spectra in the C–O stretching frequency region with 0.025% CO in argon using relatively high laser energy (6 mJ/pulse) are illustrated in Figure 1, and the new product absorptions are listed in Table 1. The stepwise annealing and photolysis behavior of these new product absorptions are also shown in the Figure 1. In addition to the strong CO absorption at 2138.4 cm^{-1} (not shown), two bands at 1907.7 and 1919.3 cm^{-1} were observed on sample deposition (trace a). Annealing to 30 K (trace b) markedly increased the 1907.7 and 1919.3 cm^{-1} absorptions and produced new absorptions at 1935.0 (several site absorptions were also observed, which are listed in the table but not mentioned here), 1815.2, 1811.7, 1804.2, and 1801.0 cm^{-1} . These absorptions kept increasing on another 34 K annealing (trace c), during which new absorptions at 2007.2, 2005.7, 1833.5, and 1831.2 cm^{-1} appeared. Subsequent broad-band irradiation (trace d) almost destroyed the 2007.2, 2005.7, 1833.5, and 1831.2 cm^{-1} absorptions, decreased the 1935.0, 1804.2, and 1801.0 cm^{-1} absorptions, slightly increased the

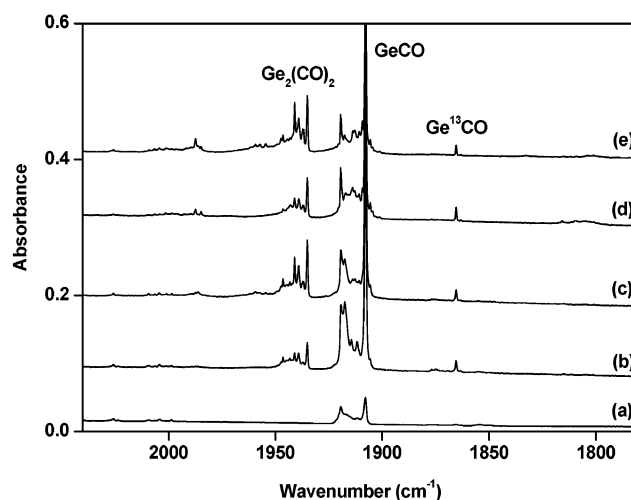


Figure 2. Infrared spectra in the 2040–1780 cm^{-1} region from co-deposition of laser-ablated germanium atoms with 0.5% CO in Ar. (a) 1 h of sample deposition at 7 K, (b) after annealing to 30 K, (c) after annealing to 34 K, (d) after 20 min of broad-band irradiation, and (e) after annealing to 38 K.

1907.7, 1815.2, and 1811.7 cm^{-1} absorptions, and produced new absorptions at 1987.3 and 1984.7 cm^{-1} . All of these new absorptions increased on a final annealing to 40 K (trace e). In addition, a weak band at 1709.2 cm^{-1} (not shown), which was previously assigned to the GeCO^- anion, also appeared on sample deposition, decreased on annealing, and disappeared on broadband irradiation.²⁴

Figure 2 shows the spectra in the C–O stretching frequency region with 0.5% CO in argon using relatively low laser energy (4 mJ/pulse). Similar to the experiment shown in Figure 1, the 1907.7 and 1919.3 cm^{-1} absorptions were observed on sample deposition, and they increased on 30 K annealing and on broadband irradiation. The 1935.0 cm^{-1} absorption appeared on 30 K annealing, increased on 34 K annealing, and decreased on broadband irradiation. The 1987.3 and 1984.7 cm^{-1} absorptions were also produced on broadband irradiation and increased on subsequent 40 K annealing. It is noteworthy that the absorptions at 2007.2, 2005.7, 1833.5, 1831.2, 1815.2, 1811.7, 1804.2, and 1801.0 cm^{-1} were not observed either on annealing or on broadband irradiation.

Different isotopic carbon monoxides, $^{13}\text{C}^{16}\text{O}$, $^{12}\text{C}^{18}\text{O}$, as well as $^{12}\text{C}^{16}\text{O} + ^{13}\text{C}^{16}\text{O}$ and $^{12}\text{C}^{16}\text{O} + ^{12}\text{C}^{18}\text{O}$ mixtures, were employed for product identification through isotopic shifts and splittings. The isotopic counterparts are also listed in Table 1. The mixed $^{12}\text{C}^{16}\text{O} + ^{13}\text{C}^{16}\text{O}$ spectra in the C–O stretching frequency region are shown in Figures 3 and 4, and the mixed $^{12}\text{C}^{16}\text{O} + ^{12}\text{C}^{18}\text{O}$ spectra in the C–O stretching frequency region are illustrated in Figure 5.

Calculation Results. Quantum chemical calculations were performed on the potential product molecules. The optimized structures are shown in Figure 6. The vibrational frequencies and intensities are listed in Table 2. Table 3 provides a comparison of observed and calculated isotopic frequency ratios for the observed vibrational modes.

GeCO. The 1907.7 cm^{-1} band is the dominant product absorption in all the experiments with different CO concentrations and laser energies. This band shifted to 1865.4 cm^{-1} with ^{13}C and to 1863.1 cm^{-1} with ^{18}O . The isotopic frequency ratios ($^{12}\text{C}/^{13}\text{C} = 1.0227$ and $^{16}\text{O}/^{18}\text{O} = 1.0239$) indicate that the band is due to the C–O stretching mode of a germanium carbonyl species. It is obviously attributed to a germanium carbonyl species containing a single CO group, since only the

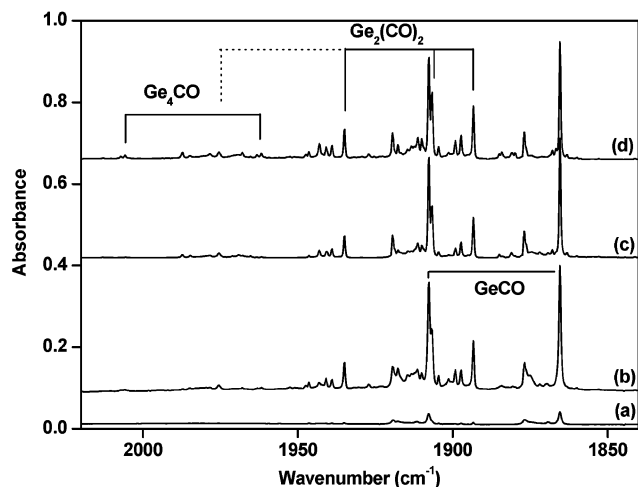


Figure 3. Infrared spectra in the 2020–1840 cm^{-1} region from co-deposition of laser-ablated germanium atoms with 0.02% $^{12}\text{C}^{16}\text{O}$ + 0.02% $^{13}\text{C}^{16}\text{O}$ in Ar. (a) 1 h of sample deposition at 7 K, (b) after annealing to 34 K, (c) after 20 min of broad-band irradiation, and (d) after annealing to 38 K.

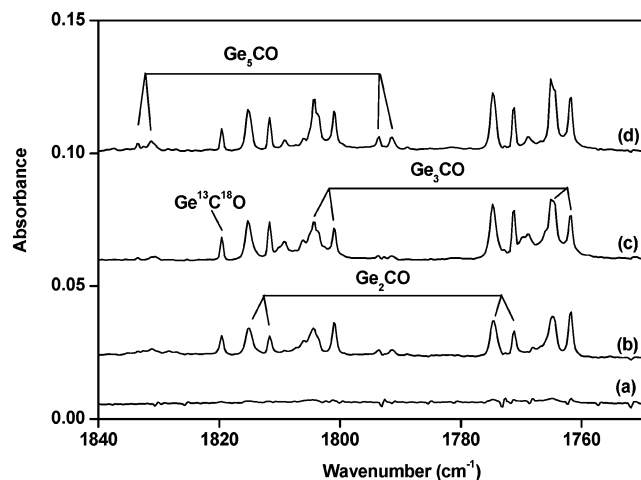


Figure 4. Infrared spectra in the 1840–1750 cm^{-1} region from co-deposition of laser-ablated germanium atoms with 0.02% $^{12}\text{C}^{16}\text{O}$ + 0.02% $^{13}\text{C}^{16}\text{O}$ in Ar. (a) 1 h of sample deposition at 7 K, (b) after annealing to 34 K, (c) after 20 min of broad-band irradiation, and (d) after annealing to 38 K.

pure isotopic counterparts were observed in the mixed $^{12}\text{C}^{16}\text{O}$ + $^{13}\text{C}^{16}\text{O}$ and $^{12}\text{C}^{16}\text{O}$ + $^{12}\text{C}^{18}\text{O}$ experiments. The 1907.7 cm^{-1} band is assigned to the GeCO molecule. The 1919.3 cm^{-1} band showed the same isotopic shifts and splittings as the 1907.7 cm^{-1} band, and it is also assigned to GeCO at a different trapping site. Cesaro and co-workers have observed GeCO at 1918.9/1907.5 cm^{-1} from thermal Ge atom reactions with CO in solid argon.¹⁶ Previous ab initio calculations predicted the GeCO molecule to have a $^3\Sigma^-$ ground state with a linear structure. The GeOC isomer was predicted to lie about 70 kJ/mol higher in energy than GeCO .¹⁶ The C–O stretching frequency of GeCO was calculated to be 1967.0 cm^{-1} with 853 km^2/mol IR intensity. The Ge–C stretching and bending modes were predicted at 397.9 and 286.4 cm^{-1} with almost zero IR intensities.

$\text{Ge}_2(\text{CO})_2$. In our most recent study on the reactions of silicon atoms and small clusters with CO in solid argon, a sharp band at 1928.7 cm^{-1} , which was previously assigned to the linear $\text{Si}(\text{CO})_2$ molecule, is reassigned to the $\text{Si}_2(\text{CO})_2$ molecule on the basis of both experimental observations and theoretical calculations.¹⁸ A similar band at 1935.0 cm^{-1} in the present

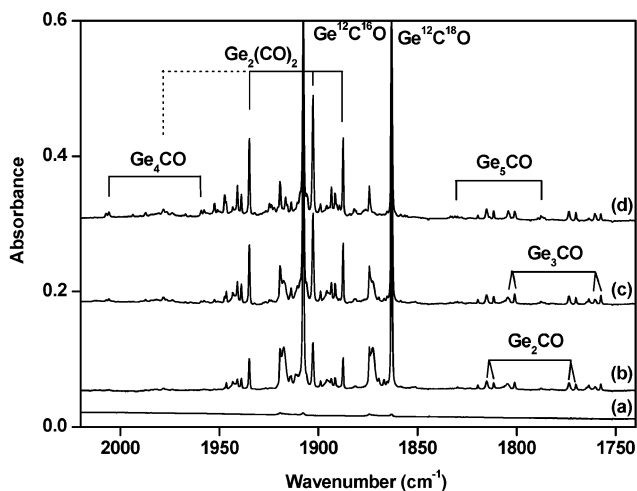


Figure 5. Infrared spectra in the 2020–1840 cm^{-1} region from co-deposition of laser-ablated germanium atoms with 0.02% $^{12}\text{C}^{16}\text{O}$ + 0.02% $^{12}\text{C}^{18}\text{O}$ in Ar. (a) 1 h of sample deposition at 7 K, (b) after annealing to 30 K, (c) after annealing to 34 K, and (d) after annealing to 38 K.

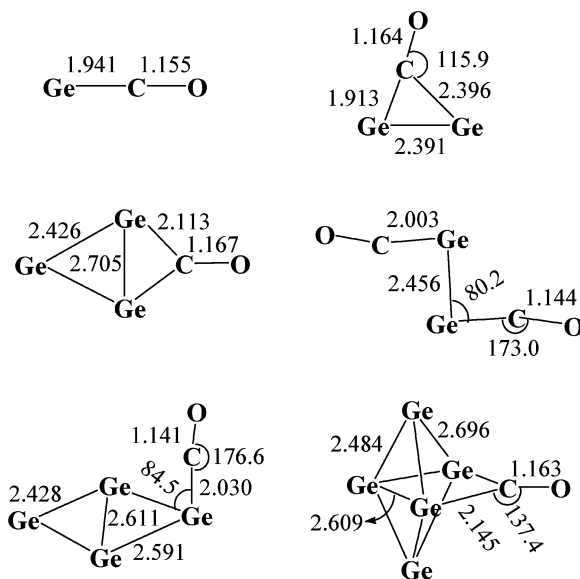


Figure 6. Optimized structures (bond lengths in angstrom, bond angles in degree) of the reaction products.

Ge + CO experiments is assigned to the $\text{Ge}_2(\text{CO})_2$ molecule following the example of $\text{Si}_2(\text{CO})_2$. As shown in Figures 1 and 2, this band appeared together with nearby matrix site-split bands at 1939.0 and 1940.9 cm^{-1} on 30 K annealing, increased on 34 K annealing, but markedly decreased on broadband irradiation. A triplet at 1935.0, 1906.7, and 1893.4 cm^{-1} was observed when a mixed $^{12}\text{C}^{16}\text{O}$ + $^{13}\text{C}^{16}\text{O}$ /Ar sample was used. A similar triplet at 1935.0, 1902.8, and 1887.6 cm^{-1} was observed in the mixed $^{12}\text{C}^{16}\text{O}$ + $^{12}\text{C}^{18}\text{O}$ spectra. These band profiles indicate that two equivalent CO subunits are involved, and the 1935.0 cm^{-1} band should be assigned to the C–O stretching mode of a $\text{Ge}_x(\text{CO})_2$ species. The observation of only one C–O stretching vibration implies that the molecule is linear or centrosymmetric. In previous thermal Ge atom reactions with higher CO concentration, a weak band at 1951.1 cm^{-1} in solid N_2 has been tentatively assigned to the $\text{Ge}(\text{CO})_2$ molecule.¹⁶ The $\text{Ge}(\text{CO})_2$ molecule was theoretically predicted to have a $^1\text{A}_1$ ground state with a bent geometry. A linear structure ($^3\Sigma_g^-$) was predicted to lie significantly higher in energy (23.5 kcal/mol) than the bent $^1\text{A}_1$ structure. Further frequency calculations revealed that the linear

TABLE 2: Calculated Harmonic Vibrational Frequencies (cm⁻¹) and Intensities (km/mol) of the Product Molecules

	frequency (intensity, mode)
GeCO	1967.0 (853, σ), 397.9 (0, σ), 286.4 (0, π)
Ge ₂ CO	1910.5 (693, a), 457.5 (24, a), 415.5 (10, a), 376.4 (2, a), 270.6 (3, a), 87.8 (1, a)
Ge ₂ (CO) ₂	2063.4 (0, a _g), 2014.9 (2298, b _u), 461.6 (0, a _g), 411.2 (13, b _u), 388.0 (1, a _u), 332.0 (0, a _g), 293.5 (48, b _u), 287.6 (0, b _g), 242.9 (0, a _g), 78.3 (0, a _g), 62.1 (2, b _u), 49.1 (1, a _u)
Ge ₃ CO	1879.5 (803, a ₁), 418.3 (0, b ₂), 395.2(1, b ₁), 314.9 (2, a ₁), 276.8 (2, a ₁), 233.3 (1, b ₂), 208.5 (12, a ₁), 179.5 (1, b ₂), 70.3 (1, b ₁)
Ge ₄ CO	2065.2 (936, a), 417.4 (20, a), 326.9 (1, a), 285.6 (10, a), 271.3 (7, a), 234.6 (2, a), 214.4 (1, a), 171.3 (1, a), 106.5 (0, a), 86.9 (2, a), 54.4 (0, a), 52.3 (1, a)
Ge ₅ CO	1902.1 (797, a ₁), 412.4 (0, b ₁), 380.5 (0, b ₂), 303.7 (1, a ₁), 262.1 (7, b ₁), 253.8 (0, a ₁), 202.1 (3, a ₁), 200.8 (0, b ₂), 186.8 (1, a ₁), 174.8 (1, b ₂), 149.5 (0, a ₂), 139.0 (2, b ₁), 117.4 (0, a ₁), 59.9 (0, b ₂), 19.5 (0, b ₁)

TABLE 3: Comparison of the Observed and Calculated Isotopic Frequency Ratios of the C–O Stretching Mode of Ge_nCO (n = 1–5) and Ge₂(CO)₂

	¹² C/ ¹³ C		¹⁶ O/ ¹⁸ O	
	obsd	calcd	obsd	calcd
GeCO	1.0227	1.0231	1.0239	1.0243
Ge ₂ CO	1.0228	1.0232	1.0235	1.0240
Ge ₃ CO	1.0222	1.0224	1.0248	1.0253
Ge ₄ CO	1.0224	1.0227	1.0245	1.0248
Ge ₅ CO	1.0222	1.0224	1.0254	1.0253
Ge ₂ (CO) ₂	1.0220	1.0224	1.0251	1.0252

structure is a transition state with an imaginary frequency. The bent ¹A₁ ground-state Ge(CO)₂ molecule was computed to have two strong C–O stretching vibrations at 1999.1 and 2071.4 cm⁻¹ with 1178:460 relative intensities. Therefore, the 1935.0 cm⁻¹ band in the present experiments cannot be assigned to the Ge(CO)₂ molecule. In previous thermal experiments, the Ge(CO)₂ molecule also was not observed in solid argon.¹⁶ Moreover, the experiments showed that the 1935.0 cm⁻¹ band is favored relative to the GeCO absorption in higher laser-energy experiments, which implies that the molecule should involve more Ge atoms than in GeCO and should be assigned to linear or centrosymmetric Ge_n(CO)₂ with $n \geq 2$.

Theoretical calculations support the assignment of the 1935.0 cm⁻¹ band to the Ge₂(CO)₂ molecule. As shown in Figure 6, the Ge₂(CO)₂ molecule was predicted to have a singlet ground state (¹A_g) with a C_{2h} symmetry. The antisymmetric C–O stretching mode (b_u) was computed at 2014.9 cm⁻¹, which should be multiplied by 0.960 to fit the observed frequency. The calculated ¹²C/¹³C and ¹⁶O/¹⁸O isotopic frequency ratios of 1.0224 and 1.0252 (Table 3) agree well with the experimental ratios of 1.0220 and 1.0251. As the molecule is centrosymmetric, the symmetric C–O stretching mode, which was predicted at 2063.4 cm⁻¹, is IR-inactive. However, this mode of the Ge₂(¹²C¹⁶O)(¹³C¹⁶O) and Ge₂(¹²C¹⁶O)(¹²C¹⁸O) isotopomers should be IR-active because of the reduced symmetry, which were calculated at 2049.3 and 2049.2 cm⁻¹ with 332 and 349 km/mol IR intensities, respectively. A weak band at 1975.4 cm⁻¹ in the mixed ¹²C¹⁶O + ¹³C¹⁶O spectra and a weak band at 1978.3 cm⁻¹ in the mixed ¹²C¹⁶O + ¹²C¹⁸O spectra tracked with the 1935.0 cm⁻¹ band are most likely due to the symmetric C–O stretching mode of the Ge₂(¹²C¹⁶O)(¹³C¹⁶O) and Ge₂(¹²C¹⁶O)(¹²C¹⁸O) isotopomers. It is possible that the 1935.0 cm⁻¹ band could originate from larger clusters, such as Ge₄(CO)₂. The most stable structure of Ge₄(CO)₂ was predicted to have a D_{2d} structure with two bridge-bonded CO units. The

IR-active C–O stretching mode was calculated at 1910.7 cm⁻¹ and does not fit the experimental value.

Ge_nCO ($n = 2-5$). In addition to the GeCO and Ge₂(CO)₂ absorptions, four doublets at 1801.0/1804.2, 1811.7/1815.2, 1831.2/1833.5, and 2005.7/2007.2 cm⁻¹ were observed in the C–O stretching frequency region. These absorptions only appeared on annealing in the experiments with lower CO concentration and higher laser energy (Figure 1). The infrared absorption spectra demonstrated unequivocally the formation of four germanium monocarbonyl species as listed in Table 1. Each doublet exhibited ¹²C/¹³C and ¹⁶O/¹⁸O isotopic frequency ratios that are characteristic of the C–O stretching vibration of a germanium carbonyl species. In the mixed ¹²C¹⁶O + ¹³C¹⁶O and ¹²C¹⁶O + ¹²C¹⁸O spectra (Figures 3–5), each doublet splits into two doublets, and obviously can be attributed to carbonyl species containing a single CO group. The products showed only the C–O stretching mode, making the definitive structure assignment difficult from the spectrum alone. However, on the basis of their growth/decay characteristics measured as a function of changes of experimental conditions, along with comparisons between the experimental observed and theoretical calculated frequencies and isotopic frequency ratios, these four doublets could be assigned to Ge_nCO with $n = 2-5$ (Tables 1).

The doublets at 1801.0/1804.2, 1811.7/1815.2, and 1831.2/1833.5 cm⁻¹ lie in the region expected for the C–O stretching vibrations of bridge-bonded carbonyl species, while the 2005.7/2007.2 cm⁻¹ doublet is due to a terminal-bonded carbonyl. The doublets at 1801.0/1804.2 and 1811.7/1815.2 cm⁻¹ appeared after the first low-temperature annealing cycle, while the doublets at 2005.7/2007.2 and 1831.2/1833.5 cm⁻¹ appeared on higher-temperature annealing. This observation implies that the 1801.0/1804.2 and 1811.7/1815.2 cm⁻¹ species involve less Ge atoms than the 1831.2/1833.5 and 2005.7/2007.2 cm⁻¹ species. Upon broadband irradiation, only the 1811.7/1815.2 cm⁻¹ doublet increased, during which the Ge₂(CO)₂ absorption decreased, suggesting that the 1811.7/1815.2 cm⁻¹ doublet should be assigned to Ge₂CO at different trapping sites.

The Ge₂ dimer has a ³Σ_g⁻ ground state. Attachment of carbon monoxide leads to a decrease in spin multiplicity. The Ge₂CO molecule was predicted to have a ¹A' ground state having a semibridge-bonded structure (Figure 6) with two inequivalent Ge–C bonds (1.913 and 2.396 Å). The most stable triplet state Ge₂CO was predicted to lie 18.4 kcal/mol above the singlet ground state. Geometry optimizations were also performed starting with end-on (C_{∞v}) and bridge-bonded (C_{2v}) structures. However, both structures were predicted to lie higher in energy than the semibridge-bonded structure and are transition states with imaginary frequencies. The Ge–Ge and C–O bond lengths of ground-state Ge₂CO are 2.391 and 1.164 Å, respectively, which are 0.017 Å shorter and 0.036 Å longer than those of Ge₂ and CO calculated at the same level. The C–O stretching vibrational frequency of ground-state Ge₂CO was computed at 1910.5 cm⁻¹. The calculated ¹²C/¹³C isotopic frequency ratio of 1.0232 and the ¹⁶O/¹⁸O ratio of 1.0240 (Table 3) are in good agreement with the observed values for the 1811.7/1815.2 cm⁻¹ doublet. The Al₂CO, Ga₂CO, and Si₂CO molecules exhibited similar C–O stretching frequencies in solid argon and were characterized to have semibridge-bonded structures.^{18,25–27}

Previous theoretical studies on Ge₃ suggested a ¹A₁ (C_{2v}) ground state, with a very low-lying ³A₂' state (D_{3h}) within 1–5 kcal/mol above.^{7,9,10} Our B3LYP/6-311+G* calculations confirmed the ¹A₁ state (C_{2v}) to be the lowest state of Ge₃, with the ³A₂' state (D_{3h}) appearing to be slightly less stable by 0.5

kcal/mol. In the case of silicon, the ground state of Si_3 was determined to be $^1\text{A}_1$ with C_{2v} symmetry both experimentally and theoretically.^{28–32} Two structures were considered when a CO molecule interacts with Ge_3 to form the Ge_3CO carbonyl. One structure is the carbon atom bridge-bonded to two Ge atoms of Ge_3 resulting in a four-membered Ge_3C ring; another structure has a Ge_3 ring with CO terminal-bonded to one of the Ge atoms. The bridge-bonded structure (Figure 6) was predicted to be the ground state of Ge_3CO , with the terminal-bonded structure lying 31.6 kcal/mol higher in energy. The C–O stretching vibrational frequency of the ground-state Ge_3CO was computed at 1879.5 cm^{-1} , slightly lower than the value predicted for Ge_2CO . The calculated isotopic frequency ratios ($^{12}\text{C}/^{13}\text{C} = 1.0224$, $^{16}\text{O}/^{18}\text{O} = 1.0253$) also support the assignment of the 1801.0/1804.2 doublet to Ge_3CO .

Previous computational studies on Ge_4 found the most stable structure to be a planar rhombus ($^1\text{A}_g$) with D_{2h} symmetry.^{9,10} Only one stable structure was found when one CO molecule attaches to Ge_4 (Figure 6). The Ge_4CO monocarbonyl was predicted to be nonplanar with C_s symmetry. The CO molecule interacts terminally with one of the apex Ge atoms of rhombus Ge_4 . The Ge_4 subunit remains nearly planar, and the CO subunit is almost perpendicular to the Ge_4 plane. Some geometry optimizations were performed starting with trial geometries without imposing any symmetry constraint. However, all of them reverted to the nonplanar C_s structure. This terminal-bonded structure has a C–O bond length of 1.141 Å, which is significantly shorter than those of bridge-bonded Ge_2CO and Ge_3CO . The C–O stretching frequency was computed at 2065.2 cm^{-1} , ca. 98.2 cm^{-1} higher than that of GeCO . The 2005.7/2007.2 cm^{-1} doublet is appropriate for the C–O stretching mode of Ge_4CO .

The remaining 1831.2/1833.5 cm^{-1} doublet is assigned to the bridge-bonded Ge_5CO molecule. This doublet is weaker than the Ge_nCO ($n = 2–4$) absorptions and is favored on higher temperature annealing. An earlier ab initio pseudopotential configuration interaction calculation suggested the ground state of Ge_5 to be a $^3\text{A}_2'$ (D_{3h}),⁸ but more recent multiconfiguration self-consistent-field and DFT/B3LYP calculations predicted a $^1\text{A}_1'$ (D_{3h}) ground state.^{9,10} Geometry optimizations were performed on the Ge_5CO monocarbonyl starting with CO either terminal-bonded to one of the Ge atom or bridge-bonded to two of the Ge atoms of Ge_5 without imposing any symmetry constraint. All of these calculations converged to a C_{2v} structure with CO bridge-bonded to two of the equatorial Ge atoms of Ge_5 (Figure 6). The C–O stretching frequency was computed at 1902.1 cm^{-1} with the isotopic frequency ratios in excellent agreement with the observed values (Table 3).

A $^1\text{A}_1$ tetragonal bipyramid structure with D_{4h} symmetry and a $^1\text{A}_1$ edge-capped bipyramidal structure with C_{2v} symmetry were previously predicted to be the lowest states for the Ge_6 cluster.^{10,12} The D_{4h} structure was predicted to be the ground state, as the previous experiments also suggested. Definitive determination of the most stable structure of the Ge_6CO carbonyl is also a difficult task. According to the bonding characters of the above assigned Ge_nCO ($n = 2–5$) clusters, geometry optimizations were performed on Ge_6CO starting with CO either terminal-bonded to one of the Ge atom or bridge-bonded to two of the Ge atoms of Ge_6 . Geometry optimization starting with the terminal-bonded structure dissociated to separated Ge_6 and CO. A minimum was found for the bridge-bonded structure, but is unstable with respect to $\text{Ge}_6 + \text{CO}$. We suggest that no stable Ge_6CO monocarbonyl species can be formed between Ge_6 and CO.

A weak doublet at 1987.3 and 1984.7 cm^{-1} appeared on broad-band irradiation and increased on higher-temperature annealing. This doublet was produced in both high and low CO concentration experiments. The band position and isotopic frequency ratios (Table 1) clearly indicate that this doublet is due to a terminal-bonded carbonyl species. This doublet could not be assigned and is simply labeled as $\text{Ge}_x(\text{CO})_y$ species in Table 1.

The B3LYP/6-311+G* calculations predicted that the CO binding energies in Ge_nCO ($n = 1–5$) are 26.9, 21.4, 25.8, 1.3, and 7.0 kcal/mol, respectively, with respect to $\text{Ge}_n + \text{CO}$. The binding energy of $\text{Ge}_2(\text{CO})_2$ with respect to $\text{Ge}_2\text{CO} + \text{CO}$ was calculated to be 13.2 kcal/mol. The binding energies of Ge_4CO and Ge_5CO were computed to be 1.6 and 7.0 kcal/mol after the basis set superposition error corrections when a more extended basis set (6-311+G(2df,2pd)) was used. The terminal-bonded Ge_4CO carbonyl is much more weakly bound than the bridge-bonded Ge_3CO and Ge_5CO molecules. Ge_4CO can be regarded as CO adsorbed on the Ge_4 cluster. The geometry of Ge_4 does not change significantly upon CO attachment. However, a Ge_3C four-membered ring structure was formed when CO bound to Ge_3 and Ge_5 clusters. The binding energies of the germanium monocarbonyls are lower than those of the corresponding silicon monocarbonyls calculated at the same level, presumably because of the larger atomic radius of germanium compared to that of silicon.¹⁸

It is interesting to note that the Ge_nCO ($n = 1–5$) species do not bind another CO to form the $\text{Ge}_n(\text{CO})_2$ species with the exception of Ge_2CO . As has been mentioned, the $\text{Ge}(\text{CO})_2$ dicarbonyl was predicted to be stable with respect to $\text{GeCO} + \text{CO}$ by about 11.6 kcal/mol. The formation of $^1\text{A}_1$ bent $\text{Ge}(\text{CO})_2$ from $^3\Sigma^-$ GeCO and CO involves spin crossing and probably requires activation energy. We also performed geometry optimization on the $\text{Ge}_3(\text{CO})_2$ species and failed in finding any stable structure with respect to $\text{Ge}_3\text{CO} + \text{CO}$.

Conclusions

Reactions of germanium atoms and small clusters with carbon monoxide molecules in solid argon have been studied using matrix isolation infrared absorption spectroscopy. In addition to the previously reported GeCO monocarbonyl, absorption at 1935.0 cm^{-1} is assigned to the antisymmetric C–O stretching vibration of $\text{Ge}_2(\text{CO})_2$ with C_{2h} symmetry. Small germanium cluster monocarbonyls, Ge_nCO ($n = 2–5$) were also produced on annealing at low CO concentrations. On the basis of isotopic substitution and theoretical calculations, absorptions at 1811.7/1815.2, 1801.0/1804.2, 1831.2/1833.5, and 2005.7/2007.2 cm^{-1} are assigned to the bridge-bonded Ge_2CO , Ge_3CO , and Ge_5CO , and terminal-bonded Ge_4CO monocarbonyls, respectively, at two trapping sites. The binding energies of Ge_nCO ($n = 1–5$) with respect to $\text{Ge}_n + \text{CO}$ were predicted to be 26.9, 21.4, 25.8, 1.3, and 7.0 kcal/mol, respectively, which are lower than those of the corresponding silicon monocarbonyls.

Acknowledgment. This work is supported by NSFC (Grant 20125311), the NKBRSF of China, and the JSPS and the NEDO of Japan.

References and Notes

- (1) Cheshnovsky, O.; Yang, S. H.; Pettiette, C. L.; Craycraft, M. J.; Liu, Y.; Smalley, R. E. *Chem. Phys. Lett.* **1987**, *138*, 119.
- (2) Arnold, C. C.; Xu, C.; Burton, G. R.; Neumark, D. M. *J. Chem. Phys.* **1995**, *102*, 6982.
- (3) Burton, G. R.; Arnold, C. C.; Xu, C.; Neumark, D. M. *J. Chem. Phys.* **1996**, *104*, 2757.

- (4) Froben, F. W.; Schulze, W. *Surf. Sci.* **1985**, *156*, 765.
- (5) Li, S.; Van Zee, R. J.; Weltner, W., Jr. *J. Chem. Phys.* **1994**, *100*, 7079.
- (6) Andzelm, J.; Russo, N.; Salahub, D. R. *J. Chem. Phys.* **1987**, *87*, 6562.
- (7) Dixon, D. A.; Gole, J. L. *Chem. Phys. Lett.* **1992**, *188*, 560.
- (8) Pacchioni, G.; Koutecky, J. *J. Chem. Phys.* **1986**, *84*, 3301.
- (9) Dai, D.; Balasubramanian, K. *J. Chem. Phys.* **1996**, *105*, 5901. Dai, D.; Balasubramanian, K. *J. Chem. Phys.* **1992**, *96*, 8345. Dai, D.; Sumathi, K.; Balasubramanian, K. *Chem. Phys. Lett.* **1992**, *193*, 251.
- (10) Archibong, E. F.; St-Amant, A. *J. Chem. Phys.* **1998**, *109*, 962.
- (11) Jo, C.; Lee, K. *J. Chem. Phys.* **2000**, *113*, 7268.
- (12) Zhao, C. Y.; Balasubramanian, K. *J. Chem. Phys.* **2001**, *115*, 3121.
- (13) Creasy, W. R.; O'Keefe, A.; McDonald, J. R. *J. Phys. Chem.* **1987**, *91*, 2848. Ray, U.; Jarrold, M. F. *J. Chem. Phys.* **1990**, *94*, 2631.
- (14) Maruyama, S.; Anderson, L. R.; Smalley, R. E. *J. Chem. Phys.* **1990**, *93*, 5349. Jarrold, M. F.; Ijiri, Y.; Ray, U. *J. Chem. Phys.* **1991**, *94*, 3607.
- (15) Jarrold, M. F. *Science* **1991**, *252*, 1085. Jarrold, M. F.; Bower, J. E. *J. Am. Chem. Soc.* **1989**, *111*, 1979.
- (16) Feltrin, A.; Cesaro, S. N.; Ramondo, F. *Vib. Spectrosc.* **1996**, *10*, 139.
- (17) Bu, Y. X.; Cao, Z. H. *J. Phys. Chem. B* **2002**, *106*, 1613.
- (18) Zhou, M. F.; Jiang, L.; Xu, Q. *J. Chem. Phys.* **2004**, *121*, 10474.
- (19) Chen, M. H.; Wang, X. F.; Zhang, L. N.; Yu, M.; Qin, Q. *Z. Chem. Phys.* **1999**, *242*, 81. Zhou, M. F.; Tsumori, N.; Xu, Q.; Kushto, G. P.; Andrews, L. *J. Am. Chem. Soc.* **2003**, *125*, 11371.
- (20) Frisch, M. J.; Trucks, G. W.; Schlegel, H. B.; Scuseria, G. E.; Robb, M. A.; Cheeseman, J. R.; Montgomery, J. A., Jr.; Vreven, T.; Kudin, K. N.; Burant, J. C.; Millam, J. M.; Iyengar, S. S.; Tomasi, J.; Barone, V.; Mennucci, B.; Cossi, M.; Scalmani, G.; Rega, N.; Petersson, G. A.; Nakatsuji, H.; Hada, M.; Ehara, M.; Toyota, K.; Fukuda, R.; Hasegawa, J.; Ishida, M.; Nakajima, T.; Honda, Y.; Kitao, O.; Nakai, H.; Klene, M.; Li, X.; Knox, J. E.; Hratchian, H. P.; Cross, J. B.; Adamo, C.; Jaramillo, J.; Gomperts, R.; Stratmann, R. E.; Yazyev, O.; Austin, A. J.; Cammi, R.; Pomelli, C.; Ochterski, J. W.; Ayala, P. Y.; Morokuma, K.; Voth, G. A.; Salvador, P.; Dannenberg, J. J.; Zakrzewski, V. G.; Dapprich, S.; Daniels, A. D.; Strain, M. C.; Farkas, O.; Malick, D. K.; Rabuck, A. D.; Raghavachari, K.; Foresman, J. B.; Ortiz, J. V.; Cui, Q.; Baboul, A. G.; Clifford, S.; Cioslowski, J.; Stefanov, B. B.; Liu, G.; Liashenko, A.; Piskorz, P.; Komaromi, I.; Martin, R. L.; Fox, D. J.; Keith, T.; Al-Laham, M. A.; Peng, C. Y.; Nanayakkara, A.; Challacombe, M.; Gill, P. M. W.; Johnson, B.; Chen, W.; Wong, M. W.; Gonzalez, C.; Pople, J. A. *Gaussian 03*, Revision B.05; Gaussian, Inc.: Pittsburgh, PA, 2003.
- (21) Becke, A. D. *J. Chem. Phys.* **1993**, *98*, 5648.
- (22) Lee, C.; Yang, E.; Parr, R. G. *Phys. Rev. B* **1988**, *37*, 785.
- (23) McLean, A. D.; Chandler, G. S. *J. Chem. Phys.* **1980**, *72*, 5639. Krishnan, R.; Binkley, J. S.; Seeger, R.; Pople, J. A. *J. Chem. Phys.* **1980**, *72*, 650.
- (24) Zhang, L. N.; Dong, J.; Zhou, M. F. *J. Chem. Phys.* **2000**, *113*, 8700.
- (25) Xu, C.; Manceron, L.; Perchard, J. P. *J. Chem. Soc., Faraday Trans.* **1993**, *89*, 1291.
- (26) Kong, Q. Y.; Chen, M. H.; Dong, J.; Li, Z. H.; Fan, K. N.; Zhou, M. F. *J. Phys. Chem. A* **2002**, *106*, 11709.
- (27) Himmel, H. J.; Downs, A. J.; Green, J. C.; Greene, T. M. *J. Phys. Chem. A* **2000**, *104*, 3642.
- (28) Raghavachari, K.; Logovinsky, V. *Phys. Rev. Lett.* **1985**, *55*, 2853. Rohlfling, C. M.; Raghavachari, K. *J. Chem. Phys.* **1992**, *96*, 2114.
- (29) Grev, R. S.; Schaefer, H. F. *Chem. Phys. Lett.* **1985**, *119*, 111.
- (30) Fulara, J.; Freivogel, P.; Grutter, M.; Maier, J. P. *J. Phys. Chem.* **1996**, *100*, 8042.
- (31) McCarthy, M. C.; Thaddeus, P. *Phys. Rev. Lett.* **2003**, *90*, 213003.
- (32) Li, S.; Van Zee, R. J.; Weltner, W., Jr.; Raghavachari, K. *Chem. Phys. Lett.* **1995**, *243*, 275.